Provided for non-commercial research and education use.
Not for reproduction, distribution or commercial use.

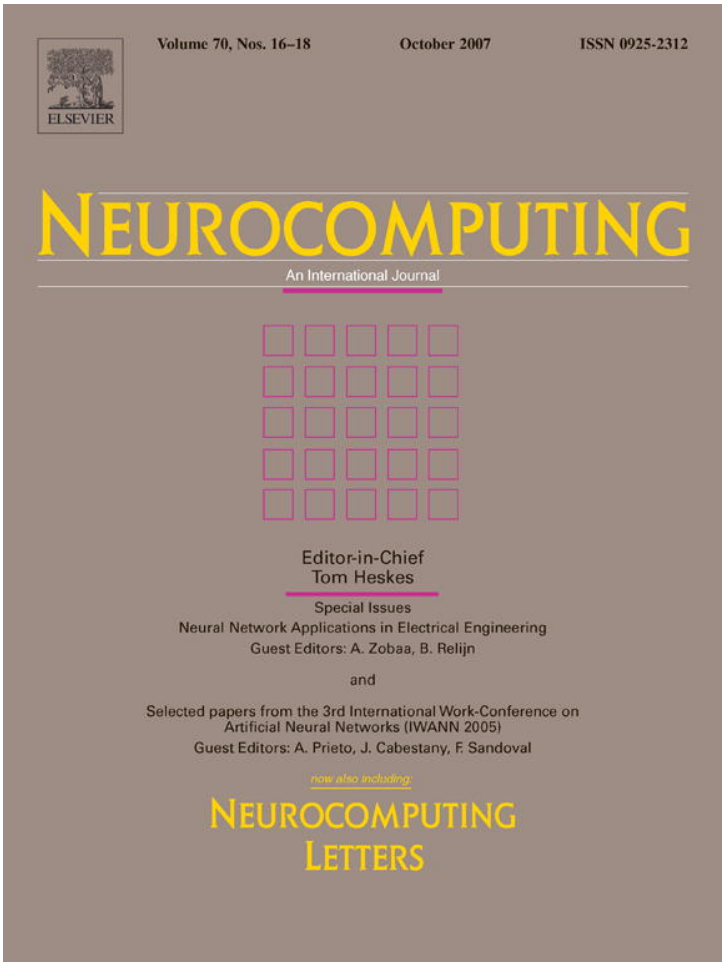

This article was published in an Elsevier journal. The attached copy is furnished to the author for non-commercial research and education use, including for instruction at the author's institution, sharing with colleagues and providing to institution administration.

Other uses, including reproduction and distribution, or selling or licensing copies, or posting to personal, institutional or third party websites are prohibited.

In most cases authors are permitted to post their version of the article (e.g. in Word or Tex form) to their personal website or institutional repository. Authors requiring further information regarding Elsevier's archiving and manuscript policies are encouraged to visit:

http://www.elsevier.com/copyright

Author's personal copy

Available online at www.sciencedirect.com
ScienceDirect
Neurocomputing 70 (2007) 2668–2678
NEUROCOMPUTING
www.elsevier.com/locate/neucom

Estimation of rotor angles of synchronous machines using artificial neural networks and local PMU-based quantities

Alberto Del Angel, Pierre Geurts, Damien Ernst, Mevludin Glavic, Louis Wehenkel*

Department of Electrical Engineering and Computer Science, University of Liege, Sart Tilman B-28, B-4000 Liege, Belgium

Available online 27 February 2007

Abstract

This paper investigates a possibility for estimating rotor angles in the time frame of transient (angle) stability of electric power systems, for use in real-time. The proposed dynamic state estimation technique is based on the use of voltage and current phasors obtained from a phasor measurement unit supposed to be installed on the extra-high voltage side of the substation of a power plant, together with a multilayer perceptron trained off-line from simulations. We demonstrate that an intuitive approach to directly map phasor measurement inputs to the neural network to generator rotor angle does not offer satisfactory results. We found out that a good way to approach the angle estimation problem is to use two neural networks in order to estimate the $\sin(\delta)$ and $\cos(\delta)$ of the angle and recover the latter from these values by simple post-processing.

Simulation results on a part of the Mexican interconnected system show that the approach could yield satisfactory accuracy for real-time monitoring and control of transient instability.
© 2007 Elsevier B.V. All rights reserved.

Keywords: Multilayer perceptrons; Transient stability monitoring and control; Phasor measurement units; Electric power systems

1. Introduction

As economic considerations continue to demand the operation of power systems closer to their stability limits, there is an increasing need for reliable and accurate means to improve security. Among these, real-time emergency control schemes, such as automatic load and generation tripping and islanding, constitute the last resort and hence most important barrier of defence against blackouts.

Power system transient (angle) stability assessment consists of evaluating the ability of the system to face various disturbances without loss of synchronism and of proposing appropriate remedial actions whenever deemed necessary [15]. To monitor and control in real-time transient stability, the rotor angle and speed of the synchronous generators are the most important reference quantities. Indeed, if these quantities can be estimated with sufficient accuracy and speed, they can be exploited in order to monitor in real-time loss of synchronism and devise automatic closed loop stabilization schemes [21].

In this paper, the approach using artificial neural networks (ANN) to estimate and predict rotor angles based on phasor measurement unit (PMU) quantities, first introduced in [3], is enhanced and investigated in depth. In order to develop a rotor angle estimator for the centre of inertia (COI) of a given power plant, this approach consists of:

1. modelling in a detailed way power plant dynamics and data acquisition devices in a simulator at the level of electromagnetic transients,
2. using the simulator off-line to generate a set of system trajectories representative of normal, during fault and post-fault behaviour in a broad range of conditions,
3. extracting from the simulation results time-series of rotor angles, voltage and current phasors provided by a PMU located at the extra-high-voltage (EHV) side of the step-up transformers of a given power plant,
4. using automatic supervised learning to train a black-box model in the form of a multilayer perceptron (MLP) to

*Corresponding author.
E-mail address: lwh@montefiore.ulg.ac.be (L. Wehenkel).

0925-2312/$ - see front matter © 2007 Elsevier B.V. All rights reserved.
doi:10.1016/j.neucom.2006.12.017

Author's personal copy

estimate from the PMU-based quantities average rotor angles of the power plant (we will refer to these as the COI dynamics of the plant).

This approach is motivated by the growing needs for real-time monitoring and control of power system transient (angle) dynamics and by the fact that PMU devices become more and more widely available on real systems (Western Energy Coordination Council, USA [1], Spain and Italy [4], Nordic countries [5], Brazil [2], Hydro—Quebec, Canada, [9,8]).

The paper is organized as follows. Section 2 defines and motivates the rotor angle estimation and prediction problem that we want to tackle in real-time and the basic principle of the proposed approach based on off-line training of MLPs. Section 3 provides details of the test power system, its simulation model and the scenarios used to validate the approach. Section 4 discusses the results of training neural networks on them. Section 5 reports on related work and investigates the potential applications of the proposed method. Section 6 draws the main conclusions and provides several directions for further research.

2. Problem formulation and principle of the proposed approach

2.1. Rotor angle estimation and prediction problem

Synchronous time frame rotor angles cannot be obtained easily by direct measurements. On the other hand, their estimation can, at least in principle, be carried out from the three-phase voltage and current phasors at the machine's low voltage bus [18]. However, given the better accuracy of EHV phasor measurements with respect to medium voltage ones, we suppose that the PMUs will in practice be installed on the EHV side of the step-up transformer of the power plant. Also, since for transient stability monitoring it is not necessary to estimate angles of individual generators [19], and because of limited observability, our scheme aims at estimating only the rotor angle of the COI of the considered power plant.

In other words, the problem to be tackled can be formulated as follows:

Given, a time-series of three-phase voltage phasors and of out-flowing (three-phase) current phasors acquired at the EHV side of a power plant, sampled at a certain rate (typically one or two cycles), and represented in a synchronous reference-frame at nominal frequency, compute an estimate of rotor angle of the centre of inertia of the power plant in the same reference-frame, and compute a prediction of this quantity at the next and subsequent time-steps.

2.2. Discussion of the proposed approach

The relationship between the above specified EHV PMU-based quantities and the actual state of the COI of the power plant is essentially non-linear and typically corrupted by measurement noise and modelling uncertainties. Therefore, we propose to use automatic learning techniques, more specifically supervised MLP training in order to provide a black-box state estimation algorithm able to cope with such difficulties.

Indeed, it is well known that neural networks, and more generally automatic learning, can cope with uncertainties and non-linearities, at least provided that the dimensionality of their input space remains moderate. Note that this is the case in the present application (see also the case study in Sections 3 and 4), since typically the number of input variables will be in the range of a few tens (at most 100) while by simulation it is possible to generate automatically a very large sample of training scenarios (typically a few thousand) yielding easily a few hundred thousand of training pairs. These scenarios can thus cover a representative sample of power system configurations, fault scenarios, modelling assumptions and they can also take into account measurement noise. Training a neural network on such very large and representative scenarios thus may presumably lead to a robust and at the same time very efficient estimation algorithm.

The approach thus essentially consists of generating off-line, and based on numerical simulations, a representative training set composed of system trajectories comprising inputs (sequences of voltage and current phasor measurements) and output sequences of rotor angles of the COI of the studied power plant. Obviously, it is of paramount importance that the set of simulation scenarios is representative of all power system configurations and fault scenarios.

It is clear that the neural network model needs to be updated when major changes occur in the power system around the studied power plant, such as new transmission or generation equipment. On the other hand, since the relationship between the COI of the power plant and PMU-based quantities depends on the number of generators in operation in the plant, we suggest to train different neural network models for each combination of generators in operation, and to use in real-time the one corresponding to the actual configuration. One could argue this is not practical due to possible combinatorial explosion of the problem. Fortunately, in practice there are few typical configurations (combination of generators in operation) and the problem would be computationally tractable. We will not further discuss these latter issues in the present paper, which merely aims at demonstrating the technical feasibility of the approach.

3. Description of case study

We describe and motivate in this section the modelling assumptions made in order to assess the feasibility of neural network based rotor angle estimation.

Author's personal copy

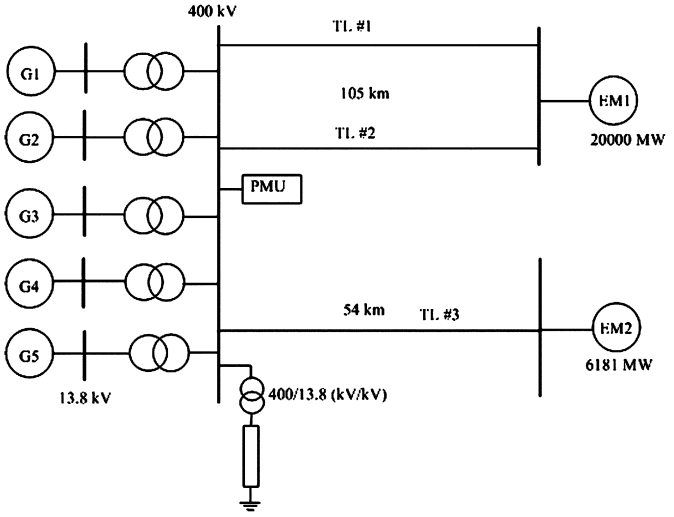

Fig. 1. Study subsystem.

3.1. Mexican interconnected system (MIS)

The bulk MIS comprises a huge 400/230 kV transmission system stretching from the border with Central America to its interconnection with the USA [14]. We focus on the south-eastern part of the MIS (illustrated by one-line diagram in Fig. 1) comprising a large hydro-power plant with five generators. This plant is connected to the remaining system by three transmission lines at 400 kV. The rest of the system is represented in a simplified way by one equivalent load located in the 400 kV bus close to the power plant and two large (equivalent) synchronous machines.

Each machine has a capacity of 190 MVA at 13.8 kV. The length of transmission lines 1 and 2 is of 105.0 km and that of transmission line 3 is of 54 km. The PMU device was placed in the 400 kV bus closest to the studied hydro-plant (see Fig. 1).

The objective of our simulations is thus to train a neural network estimator of the COI dynamics of the study plant using as inputs the current and voltage phasors obtained from this PMU.

3.2. System configurations and disturbances

In order to train a neural network model that is general enough to cope with different operating states of the system (but fixed number of generators in operation in the power plant), we considered four different levels of generation of the power plant (see Table 1). Similarly, three network topology cases were taken into account, named, respectively, Base Case, Case Five (impedances of transmission lines increase by 5%) and Case Ten (impedances of transmission lines decrease by 10%).

The generation level was changed using the hydro-governor control, and the load values where kept constant, while the two equivalent machines supply the active and reactive power balance.

Table 1
Active and reactive power for the power plant

Level generation (%)	Active power (MW)	Reactive power (MVAR)
100	190.1	−25.98
90	170.9	−24.17
80	151.9	−27.89
70	132.8	−27.95

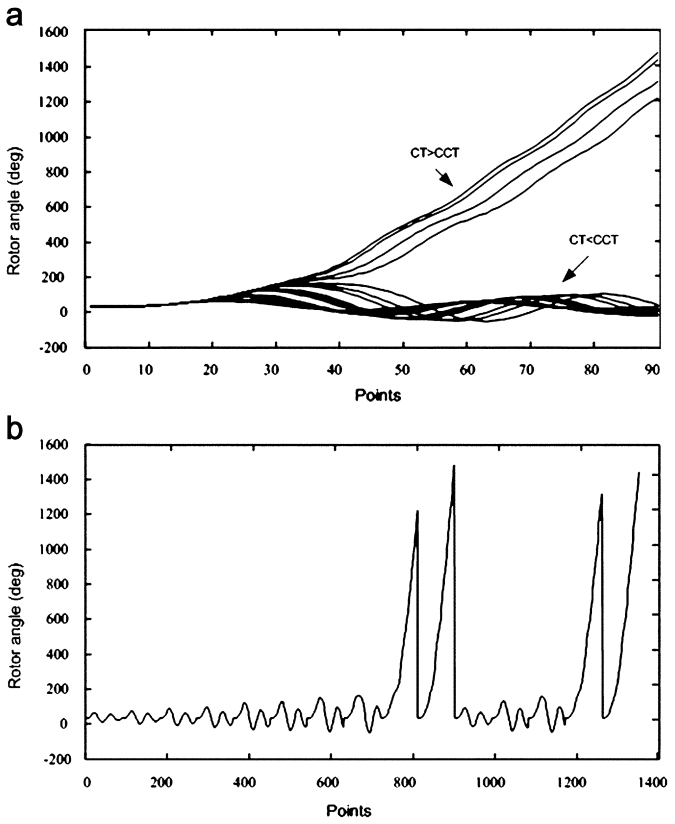

Fig. 2. Data generated (a) and the data presented to the neural network (b).

Since we do not want our scheme to rely on the disturbance detection and identification in real-time, we considered various single- and three-phase faults applied at the bus near the power plant, cleared by self-extinction, by permanent tripping of the faulted line (either line 1 or line 3), or by tripping followed by re-closing the faulted line. The critical clearing time (CCT) was calculated and different fault clearing times were selected in order to obtain stable and unstable cases. For each generation level, topology condition and fault assumption, we generated 20 different simulation scenarios around the corresponding CCT. Data generated are illustrated in Fig. 2a and their presentation to the neural network in Fig. 2b (one point corresponds to a sample of PMU quantities supposed to be collected every 0.017 s or every cycle of base system frequency of 60 Hz). CCT time chosen is 0.30 s (scenarios

Author's personal copy

are generated by choosing randomly different values of the fault clearing around the CCT, in order to generate unstable (CT > CCT) and stable scenarios (CT < CCT), generation level is 100% (base case) and with the fault applied at the beginning of the line TL #1 cleared by self-extinction.

Overall these variants yielded a total number of 1300 simulation scenarios used to build training and testing samples.

3.3. Power system dynamics and PMU model used in the simulation

Synchronous machines are represented by hydraulic generator model with one damper winding in the q-axis. The subtransient model of eighth order [13] was used and parameters of the machines for the particular system under study are given in Appendix. The exciter is based on an IEEE type SCRX solid-state exciter with parameters as in Appendix. The turbine model is the IEEE type 'Non-Elastic Water Column' without surge tank, while the model of the hydro-governor is of the mechanical-hydraulic control type [13]. The transmission lines were modelled using a simple couple PI section model (parameters given in Appendix). Loads are represented as a function of voltage magnitude and frequency [13].

To carry out the simulations, we used the PSCAD software, which is a graphical user interface to the EMTDC solution engine [13]. EMTDC is a simulation tool which differs from phasor domain solution engines, such as load-flow and transient stability programs, which utilize steady-state equations to represent electrical circuits. EMTDC simulations are solved as instantaneous values in time, yet can be converted into phasor magnitudes and angles via transducer and measurement functions provided in PSCAD—similar to the way real system measurements are performed. Although, the EMTDC simulation comes with a very high computational burden, it allows one to take into account more accurately than transient stability simulations the dynamic behaviour of electrical quantities during and after the occurrence of the fault, especially in unbalanced conditions which are typical of real-life.

PMU is a power system device that provides measurements of real-time phasors of bus voltage and line currents. Basically, it samples (same-time sampling) input voltage and current waveforms using a common synchronizing signal from the global positioning satellite, GPS [17], and calculates a phasor (magnitude and angle, see Fig. 3a) via Discrete Fourier Transform (DFT) applied on a moving data window whose width can vary from fraction of a sine wave cycle to multiple of the cycle [17,7]. The capabilities of a PMU are illustrated in Fig. 3b. The measurement set is composed of the bus voltage magnitude V_B and angle θ_B, as well as the line and injection currents magnitude and angles $I_1, I_2, I_3, I_L, \theta_1, \theta_2, \theta_3$ and θ_L.

PSCAD provides a time domain voltage and current waveform similar to what can be measured on the power system. In order to model the PMU device, the time domain waveform must be converted to a phasor equivalent. Within PSCAD there are RMS measurement blocks and three-phase on line DFT processing blocks that can provide the magnitudes and phase angle of the fundamental frequency as a function of time. The input signals are first sampled before they are decomposed into harmonic constituents.

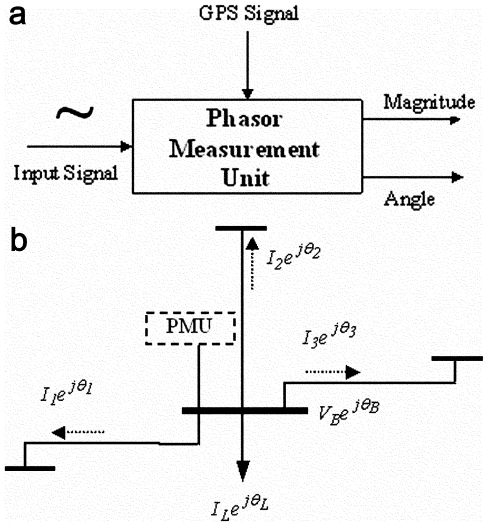

Fig. 3. Phasor measurement unit: simplified functional view (a) and capabilities (b).

In the dynamic simulations we used a time step of 50 ms and a simulation window of 1.5 s for each scenario. From these, time-series were sub-sampled at the rate of 1 sample every cycle (16.6 ms), yielding a batch of 90 samples per scenario and a total number of 117 000 (90 times 1300) samples.

4. MLP training results

4.1. Neural networks model and training algorithm

We used MLPs (see Fig. 4) with one or two hidden layers and variable numbers of neurons in each layer. The structure of MLPs and number of units in the hidden layers are determined experimentally, from studying the network behaviour during the training process taking into consideration some factors like convergence rate, error criteria, etc. In this regard, different configurations were tested and the best suitable configuration (MLPs with one or two hidden layers) was selected based on the accuracy level required. We used hyperbolic tangent activation functions for the hidden neurons and linear ones in the output layer. The MLPs were trained in batch-mode, using Levenberg–Marquard algorithm [6], and without regularization, as implemented in the PEPITo data mining software (versions 1.4 and 1.5 [16]). Prior to neural network training, the inputs and outputs are automatically normalized by withdrawing the average value and dividing

Author's personal copy

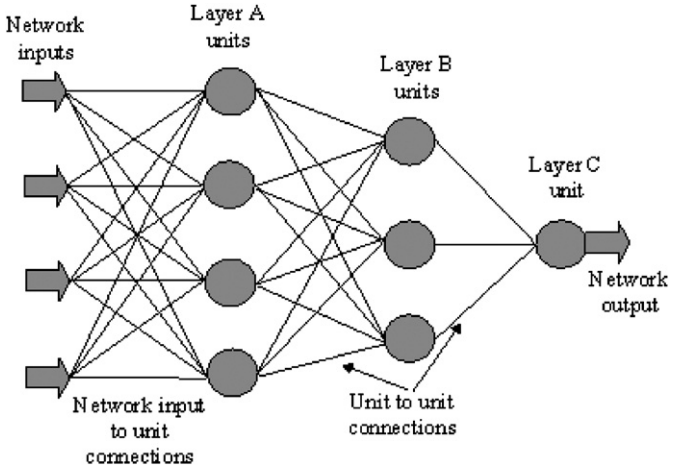

Fig. 4. Multilayer perceptron (with two hidden layers).

them by their standard deviation (both are computed on the training set).

4.2. Data preparation

The PSCAD simulations generate for each scenario a system trajectory from which the files that the PEPITo software can read are extracted, and comprising all the inputs and outputs to be used in the training and testing of the neural network. Basically, each time step of each scenario will yield a corresponding input/output pair. To construct such an input output pair, for the purpose of rotor angle estimation, the variable used as output is rotor angle ($\delta(t)$) at the current time step. On the other hand, the variables used as inputs are three-phase voltages at the bus where PMU is located, currents flows of the three transmission lines, current towards the local load, at the current time step, and also at the two previous time steps [3]. This leads to a maximum number of 90 input variables listed in Table 2.

The set of scenarios was split into 980 training scenarios and 320 testing scenarios, yielding a training set of 88 200 samples and a testing set of 28 800 samples, each one described by 90 instantaneous input values and 1 output. In the results reported below, the training scenarios corresponded to the different combinations of plant operating state, topology configurations and fault scenarios, and various fault clearing times below and above the CCT. The test scenarios correspond to the same configurations and faults, simulated with different fault clearing times (stable and unstable ones).

4.3. Discussion of results

4.3.1. MLPs trained on three-phase and single-phase faults

Since all the scenarios are used in these simulations, the size of learning set is 88 200 objects and we use 28 800 objects for the test set, and since some of the faults are single-phase ones, we used as inputs all the 90 variables given in Table 2. The output is the rotor angle.

Table 2
90 quantities used as inputs in the NN training

$k-2$			$k-1$			k		
V_a	V_b	V_c	V_a	V_b	V_c	V_a	V_b	V_c
θ_a	θ_b	θ_c	θ_a	θ_b	θ_c	θ_a	θ_b	θ_c
I_{1a}	I_{1b}	I_{1c}	I_{1a}	I_{1b}	I_{1c}	I_{1a}	I_{1b}	I_{1c}
θ_{1a}	θ_{1b}	θ_{1c}	θ_{1a}	θ_{1b}	θ_{1c}	θ_{1a}	θ_{1b}	θ_{1c}
I_{2a}	I_{2b}	I_{2c}	I_{2a}	I_{2b}	I_{2c}	I_{2a}	I_{2b}	I_{2c}
θ_{2a}	θ_{2b}	θ_{2c}	θ_{2a}	θ_{2b}	θ_{2c}	θ_{2a}	θ_{2b}	θ_{2c}
I_{3a}	I_{3b}	I_{3c}	I_{3a}	I_{3b}	I_{3c}	I_{3a}	I_{3b}	I_{3c}
θ_{3a}	θ_{3b}	θ_{3c}	θ_{3a}	θ_{3b}	θ_{3c}	θ_{3a}	θ_{3b}	θ_{3c}
I_{load}	I_{load}	I_{load}	I_{load}	I_{load}	I_{load}	I_{load}	I_{load}	I_{load}
θ_{load}	θ_{load}	θ_{load}	θ_{load}	θ_{load}	θ_{load}	θ_{load}	θ_{load}	θ_{load}

The first MLP configuration used had the form $90-X-\delta$, where X denotes the number of hidden neurons (respectively, of 5, 15, and 20), and the output neuron targets the rotor angle, δ. Table 3 summarizes a subset of the results obtained after training. A subset of the results obtained while using two hidden layers, are shown in Table 4. Notice that the mean square error (MSE) values displayed in these tables correspond to the normalized outputs of the neural network, while the minimum and maximum errors are displayed in degrees.

Overall, the simulations reported in the last line of Table 4 are representative of the best results obtained in this first set of simulations. For this case the (normalized) MSE is 0.007462 on the test set, which corresponds to a standard deviation of the rotor angle estimation error of about 27°. This high standard deviation, together with the very large minimum and maximum errors, leads to the conclusion that these results are not accurate enough for practical use, i.e. for reliable monitoring or transient stability.

4.3.2. MLPs trained only on three-phase faults

In order to handle a simpler problem, hoping to increase accuracy, we next focused on three-phase faults only for training and testing the neural network. In this context, it is not necessary to take into account all 90 inputs, since the values from one of the three phases (we chose phase A) are already providing all the information. This allowed us to decrease the number of input nodes down to 30 units, while the output layer still targets the value of the rotor angle, δ. Notice that restricting to the scenarios corresponding to three-phase faults, the size of learning and test sets were reduced to 43 200 and 14 400 samples. Results are summarized in Table 5, for the case of a single hidden layer of 7 or 10 units, and in Table 6, for the case of two hidden layers.

Finally, a further set of simulations were obtained by further reducing the input variables to the neural nets, by using the magnitude and phase angle of voltage measurements of phase A, and only the current magnitudes as

Author's personal copy

Table 3
Results using $90-X-\delta$ configuration (angles in degrees)

MLP configuration	MSE (ls)	MSE (ts)	Correlation factor (ts)	Error min (ts)	Error max (ts)	Cycles
$90-5-\delta$	0.1014	0.1248	0.9032	−732.44	1.19E3	50
$90-15-\delta$	0.03567	0.0475	0.9644	−717.16	870.14	50
$90-20-\delta$	0.01964	0.0277	0.9796	−461.77	568.24	50
$90-20-\delta$	0.01134	0.0192	0.9857	−682.90	529.00	100

Table 4
Results using $90-X-X-\delta$ configuration (angles in degrees)

MLP configuration	MSE (ls)	MSE (ts)	Correlation factor (ts)	Error min (ts)	Error max (ts)	Cycles
$90-10-10-\delta$	0.00546	0.0113	0.9916	−714.58	620.57	80
$90-15-15-\delta$	0.00329	0.0081	0.9940	−455.62	510.069	70
$90-18-18-\delta$	0.00241	0.0075	0.9945	−577.77	575.212	100

Table 5
Results using $30-X-\delta$ configuration (angles in degrees)

MLP configuration	MSE (ls)	MSE (ts)	Correlation factor (ts)	Error min (ts)	Error max (ts)	Cycles
$30-7-\delta$	0.01434	0.02090	0.9838	−539.89	771.77	150
$90-10-\delta$	0.02140	0.03070	0.9762	−533.02	696.04	100

Table 6
Results using $30-X-X-\delta$ configuration (angles in degrees)

MLP configuration	MSE (ls)	MSE (ts)	Correlation factor (ts)	Error min (ts)	Error max (ts)	Cycles
$30-25-5-\delta$	0.002348	0.00665	0.9949	−190.52	538.70	100
$30-25-25-\delta$	0.002729	0.00720	0.9945	−487.48	439.01	150
$30-20-5-\delta$	0.003098	0.00852	0.9935	−271.35	495.16	100

Table 7
Results using $18-X-X-\delta$ configuration (angles in degrees)

MLP configuration	MSE (ls)	MSE (ts)	Correlation factor (ts)	Error min (ts)	Error max (ts)	Cycles
$18-20-10-\delta$	0.002299	0.005969	0.9954	−191.69	480.69	250
$18-20-20-\delta$	0.001962	0.005391	0.9959	−154.30	526.39	200
$18-30-10-\delta$	0.0020	0.00551	0.9958	−282.29	481.23	250

inputs to the neural network. Current phase angles were thus not used for this configuration, leading to 18 input variables. The best results were again obtained with two hidden layers and are displayed in Table 7.

As one can see from these results, this simplification only marginally improved accuracy, which still remains below expectations. To further highlight this, Figs. 5 and 6 provide some graphical comparisons of actual rotor angle and those obtained from the neural network estimations. These latter show some very large peaks appearing at random places during the transients.

4.3.3. Use of rectangular representation of the rotor angle

We explain the difficulty to obtain accurate results in the direct estimation of rotor, angles as carried out in the previous sections, by the fact that these rotor angles

Author's personal copy

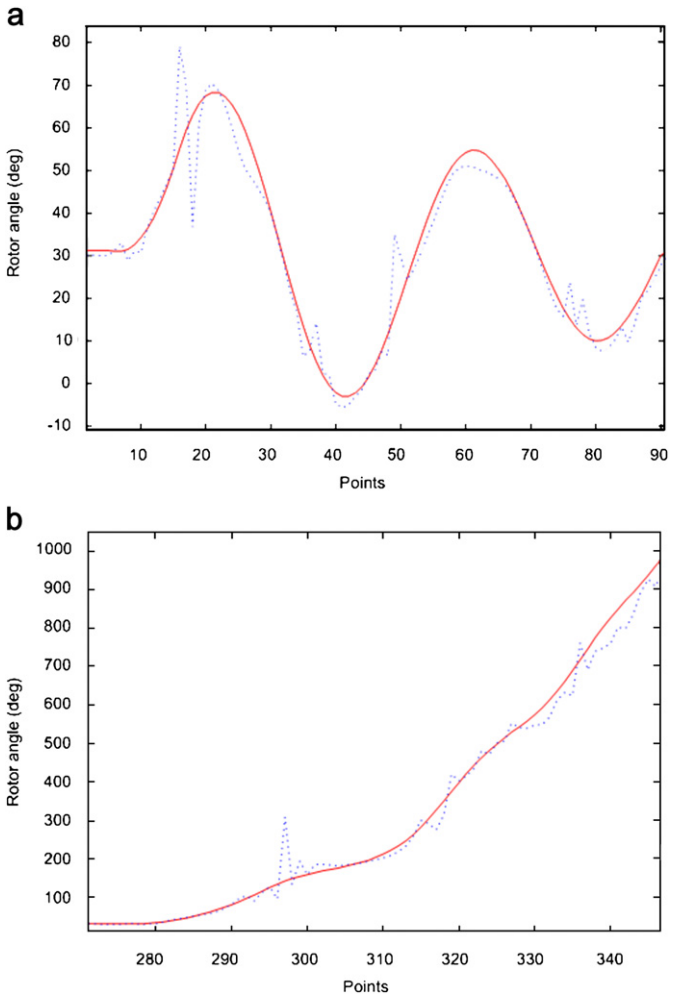

Fig. 5. True vs. estimated rotor angle for MLP 90−18−18−δ. Stable (a) and unstable (b) test scenario.

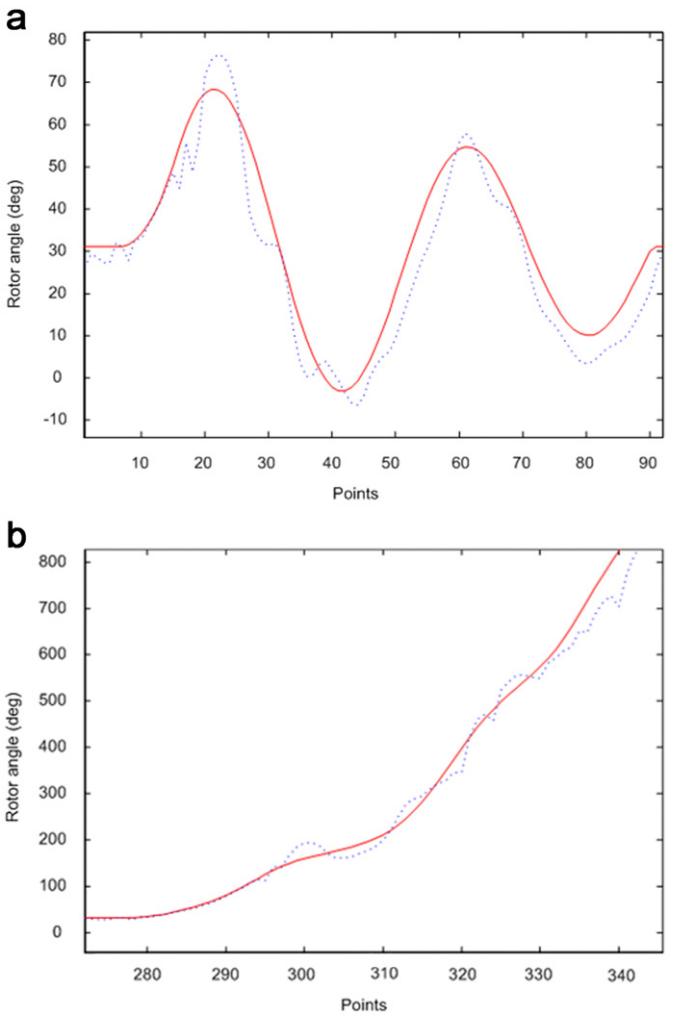

Fig. 6. True vs. estimated rotor angle for MLP 18–18–18–δ. Same stable (a) and unstable (b) test scenarios as in Fig. 5.

become quite large in the context of unstable scenarios (actually unbounded), while the phases and amplitudes of the phasor measurements used as inputs to the neural networks remain bounded (phases within the interval $[-180°, 180°]$, amplitude between 0 and some upper bound fixed by system parameters). This makes it difficult, if not impossible, to yield an estimation scheme using a limited number of past measurements to provide good accuracy both for the large excursions (over 1000°) of the rotor angle in unstable cases and the smaller variations (typically 10°−80°) in stables ones. We believe that the training of the MLPs in such conditions actually leads to overfitting the unstable scenarios at the price of a rather bad approximation of the stable ones, as suggested by Figs. 5 and 6.

In order to circumvent this problem, we propose to use instead of the direct estimation of the rotor angle δ, an indirect scheme where two neural nets are trained in parallel, in order to, respectively, provide an approximation of $\sin(\delta)$ and $\cos(\delta)$. Indeed, these values have the advantage of remaining bounded even in unstable conditions, and at the same time they vary smoothly over time. On the other hand, the rotor angle can be straightforwardly recovered from these values (up to a multiple of 360°).

Table 8 shows training and testing results obtained for two such MLPs, both with two hidden layers of eight neurons each, and a linear output neuron. In these simulations we considered only the three-phase faults of Section 4.3.2, with the same training and testing scenarios. Notice that in the present case we also decided to drop from the 30 input variables the values corresponding to $t-1$ cycle, since we found that they did not bring a significant amount of information (thus the MLPs use only 20 inputs). In order to recover the rotor angle from the approximations of $\sin(\delta)$ and $\cos(\delta)$, we used the two MLPs obtained after 150 cycles of training, which corresponded to convergence of the MSE both on the training and on the testing samples. Notice that no overfitting is observed with these structures and input and output variables (see Table 8).

Compared to the previous results we obtained a significant increase in accuracy when using this approach

Author's personal copy

Table 8
Results of training and testing MLPs with rectangular representation of δ

MLP configuration	MSE (ls)	MSE (ts)	Correlation factor (ts)	Error min (ts)	Error max (ts)	Cycles
20−8−8− sin(δ)	0.004229	0.005422	0.9951	−0.593	0.586	50
20−8−8− sin(δ)	0.003219	0.004265	0.9962	−0.563	0.495	100
20−8−8− sin(δ)	0.003118	0.005422	0.9962	−0.546	0.474	150
20−8−8− cos(δ)	0.001957	0.002743	0.9976	−0.352	0.331	50
20−8−8− cos(δ)	0.001378	0.002121	0.9982	−0.510	0.323	100
20−8−8− cos(δ)	0.001205	0.001840	0.9984	−0.547	0.335	150

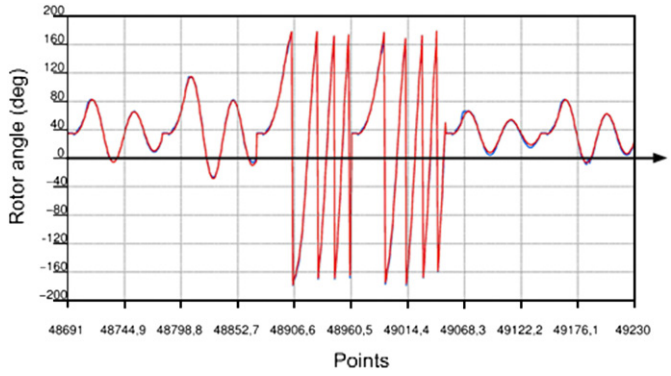

Fig. 7. Rotoror angle vs. estimation for 6 test scenarios (2 stable, 2 unstable, 2 stable). In red, the value of δ obtained from PSCAD simulations; in blue, the value computed from the 20–8–8–sin(δ) and 20–8–8–cos(δ) trained for 150 cycles.

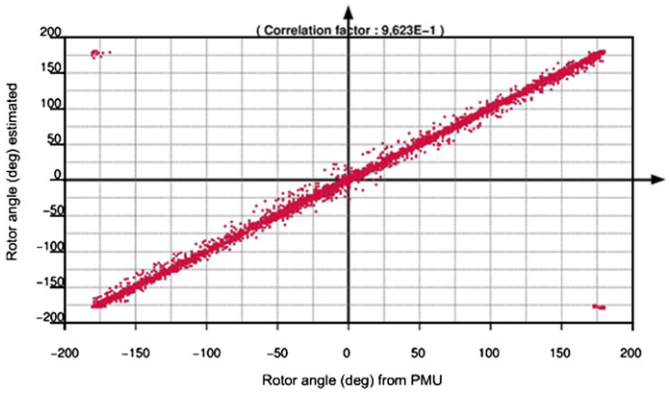

Fig. 9. Rotor angle vs. estimation for all 14 400 test samples. The points in the upper left and lower right corner correspond to 49 large instantaneous errors. Removing these points from the statistics leads to a correlation coefficient of 0.9992.

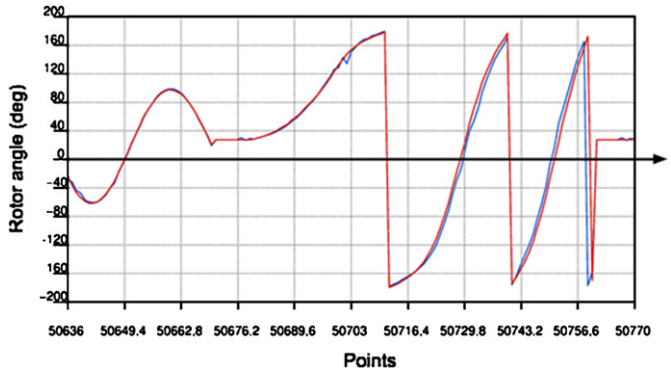

Fig. 8. Rotor angle vs. estimation for a stable followed by an unstable test scenario. The fact that the switching from $+180^\circ$ to -180° does not always happen exactly at the same time leads to approximation errors of about 360°.

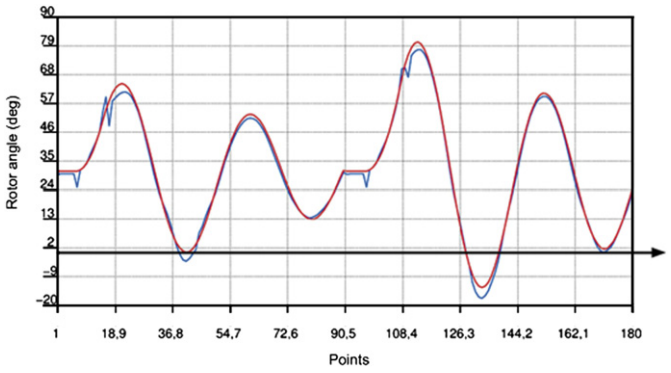

Fig. 10. Rotor angle vs. estimation for all the two first training scenarios. The discontinuities in the blue curve (estimation by MLP) correspond to fault appearance and clearing.

to estimate the rotor angle. Indeed, except for a small number of large errors (they are discussed further below), the approximation provides a standard error (on the test sample) of 3.73°, with minimum and maximum errors of, respectively, -32.4° and 26.5°. The good quality of this estimation scheme is illustrated in Figs. 7–10.

Fig. 7 shows for a few test scenarios both the true (i.e. taken from the simulations) rotor angle (in blue), and the approximation recomputed from the two MLP outputs (in red). Both are trimmed to the interval $[-180^\circ, 180^\circ]$.

Fig. 8, on the other hand, illustrates the fact that sometimes there remain large errors, but we see that these are merely due to the fact that the signal discontinuity at 180° does appear at two different (but successive) time steps for the true signal and its estimation. Although such

Author's personal copy

errors appear as large and influence the accuracy statistics in a negative way, from a practical point of view they are not problematic since they would lead to small errors in angle differences. Fig. 9 further highlights the overall performances by a scatter-plot representing the true angle and its estimation for all the 14 400 test samples. It shows that, except for 'large' errors, the approximation is of very good quality.

Finally, we illustrate in Fig. 10 two training scenarios (the two first in our data set), showing some small estimation errors at fault application and clearing instants. These small peaks of limited amplitude of one or two samples are typical errors incurred by this scheme. We deem that this kind of estimation error could also be easily detected and corrected in real time, taking advantage of the fact that rotor angles must vary smoothly.

4.3.4. Extension to rotor speed estimation and rotor angle and speed prediction

The presented approach can be extended in a straightforward way to the estimation of rotor speeds (by substituting $\omega(t)$ for $\delta(t)$, in the data preparation step) and to the prediction of one or several time steps ahead in time (by substituting $\omega(t+\Delta t)$, or $\delta(t+\Delta t)$ for $\delta(t)$, in the data preparation step). Further research will aim at assessing how accurately it is possible to predict these angles and speeds with sufficient accuracy by the same methodology.

5. Related work and potential applications

Tracking the state of the system immediately following a transient event to select an appropriate remedial control action is an emerging application of PMU technology. Indeed, since the rotor angles and speeds of the synchronous generators are the most important quantities in power system transient stability assessment and control, wrong rotor angles and speeds may result in wrong transient stability prediction and determination of control actions. Thus, accurate estimation of these two quantities is of paramount importance in considering such assessment and control scheme.

Several power utilities are already using PMUs for disturbance registration, security monitoring and emergency control [1,4,5,2,9,8]. A possible use of PMU measurements can be made to predict a developing transient and initiating important relays, or other control actions such as generation tripping [19,10,11], load shedding [19], and FACTS (flexible AC transmission system) devices [19,10,11]. A fuzzy hyper-rectangular composite neural network, which utilizes real-time phasor angle measurements to provide fast transient stability prediction, is presented in [12]. In [18] two methods for solving the real-time prediction problem are presented, solving the model forward in time in order to predict future behaviour and solving the model faster than real-time if computational resources permit. Both methodologies [18,12] rely on the so-called classical generator model and relate phasors to equivalent reactances (step-up transformer, generator) to determine rotor angles.

In more general situations phasor measurements are not taken directly from generator buses. In this case, for algebraic relation of measured voltages and the generator (internal) voltages and currents, the reduced admittance matrix can be solved for the generator internal voltages [18].

An important observation is that the use of simplified generator model together with simple algebraic relations of phasor measurements and generator angle and speed requires a priori knowledge of system parameters or reduced admittance matrix whose entries may experience changes over time and reliable system parameter identification might be required. In addition, extremely rapid acquisition of breakers status (topology changes) is required.

The discussion attached to [18] raised the very important issue of accurate synthesis of rotor angles from phasor measurements obtained by a PMU placed at the EHV side of step-up transformer.

The novelty of the approach advocated in this paper is that it does not rely on simplified generator model and thus could allow to obtain more accurate synchronous generator angle and speed estimations which would allow its application to real-life systems.

An appealing potential application of the proposed scheme is in designing system protection schemes [4,10]. Traditionally, these schemes are designed to detect abnormal system conditions and initiate pre-planned remedial control actions (generation tripping, load shedding, system separation, etc.). However, conventional system protection schemes may result in risk to system reliability by failure to operate when required and nuisance tripping when unintended [20]. To increase meaningful decisions of system protection schemes, the precise knowledge of the current state of the power system must be acquired in real-time. A system protection scheme based on PMU technology, classical generator model for generator angle and speed prediction and one-machine infinite bus transformation has been investigated in [20].

Proposed angle and speed estimation scheme, in conjunction with single machine equivalent method [15] for transient stability assessment and generation tripping as control actions, has been envisioned, and initial investigations using simple academic power system example have been performed [3] within the European Union funded project EXaMINE [4].

This paper reports on the extension of proposed scheme with application to a part of real-life power system. Further work will focus around full implementation of envisioned system protection scheme.

Author's personal copy

6. Conclusions

This paper has investigated a possibility for the estimation of rotor angles, in the time frame of transient stability, which uses only locally available quantities from a PMU device installed in the EHV part of the substation close to the power plant. The scheme is based on the off-line training a neural network approximation structure. The approach has been validated on a part of real power system model and using a very detailed time domain simulation model, for the sole case of rotor angle estimation. We found out that a good way to approach the angle estimation problem is to use two neural networks in order to estimate the $\sin(\delta)$ and $\cos(\delta)$ of the angle and recover the latter from these values by simple post-processing.

While the off-line training stage is rather time consuming, the use of the artificial neural network in real-time mode is ultra-fast. In practice, for a transient stability limited power system, we suggest to install a PMU device close to each power plant which could lose synchronism, and broadcast to them a reference phase measurement from a PMU installed close to the load centre. Thus each power plant could monitor and predict its relative motion with respect to the rest of the system and detect whenever there is a risk of loss of synchronism, so as to trigger generation tripping.

In order to make the scheme acceptable for practical use, further work is required, first in order to assess the ability of prediction sufficiently far ahead in time in order to comply with the very strict speed requirements of transient stability emergency control. Also, the impact of imperfections of measurement transformers (current and voltage) which were not taken into account in our simulations should be assessed carefully, and more systematic simulations with different types of neural networks or other automatic learning methods could be carried out in order to further optimize the accuracy and speed of the estimation and prediction algorithm.

Another very valuable, if not necessary, step of further validation would consist of using real data collected from a real system in order to assess the validity of the simulation based scheme, for example using a micro-network model with actual synchronous machines of reduced size. This is probably necessary before such a scheme could be accepted for closed loop emergency control; nevertheless, for monitoring in open loop, we believe that the scheme could be used without such simulations. We also believe that the ideas presented and benefiting from emerging sensing, communication and computing technologies, will lead to practical implementations capable of dealing with very large power systems.

Acknowledgements

The authors would like to thank PEPITe company (www.pepite.be) for gracefully providing the PEPITo software for this research. Pierre Geurts, Damien Ernst and Mevludin Glavic acknowledge the support of the Belgian National Fund for Scientific Research (FNRS). Alberto Del Angel acknowledges the support from the Instituto Politecnico Nacional (IPN) of Mexico, Programa de Superacion Academica (SUPERA) and the Comision de Operacion y Fomento de Actividades Academicas (COFAA-IPN) of Mexico.

Appendix

Here we provide the parameters of the system studied in this paper. The parameters are given in Tables 9, 10 and 11.

Table 9
Parameters of synchronous machine for the MIS test system

S	191 MVA
V	13.8 kV
f	60 Hz
T'_{do}	5.2 s
T''_{do}	0.029 s
T''_{qo}	0.034 s
H	4.3 MWs/MVA
D	1.0 p.u.
X_d	0.75 p.u.
X_q	0.43 p.u.
X'_d	0.24 p.u.
X''_d	0.17 p.u.
X''_q	0.17 p.u.
X_l	0.11 p.u.

Table 10
Parameters of the excitation system SRCX

T_A	1.02 s
T_B	15.0 s
K	220.0
T_E	0.03 s
E_{MIN}	−3.0 p.u.
E_{MAX}	4.2 p.u.

Table 11
Transmission lines parameters for the MIS test system

Parameter	TL # 1	TL # 2	TL # 3
f	60.0 Hz	60.0 Hz	60.0 Hz
V_{LL} rated	230.0 kV	230.0 kV	230.0 kV
MVA	100.0 MVA	100.0 MVA	100.0 MVA
R	0.0013 p.u.	0.0016 p.u.	0.0041 p.u.
X	0.0177 p.u.	0.0216 p.u.	0.0599 p.u.
B	0.5072 p.u.	1.6181 p.u.	1.417 p.u.

Author's personal copy

References

[1] Bonneville Power Administration, WAMS Final Report, BPA, 1999.
[2] I.C. Decker, J.G. Ehrensperger, M.N. Agostini, A.S. De Silva, A.L. Bettiol, S.L. Zimath, Synchronized phasor measurement system: development and applications, in: Proceedings of IX Symposium of Specialists in Electric Operational and Expansion Planning (SEPOPE), Paper SP-086, Rio de Janeiro, Brasil, 2004.
[3] A. Del Angel, M. Glavic, L. Wehenkel, Using artificial neural networks to estimate rotor angles and speeds from phasor measurements, in: Proceedings of Intelligent System Applications in Power ISAP2003, Lemnos, Greece, Paper ISAP03/017, 2003.
[4] A. Diu, L. Wehenkel, EXaMINE—experimentation of a monitoring and control system for managing vulnerabilities of the European infrastructure for electric power exchange, in: Proceedings of IEEE/PES Summer Meeting, Chicago, USA, 2002.
[5] ELORSK: wide area measurements of power system dynamics—the North American WAMS project and its applicability to the Nordic countries, ELFORSK, Lund, Sweden, 2000.
[6] S. Haykin, Neural Networks, A Comprehensive Foundation, IEEE Press, New York, 1994.
[7] IEEE 1344, Standard for synchrophasors for power systems, New York, 1995.
[8] I. Kamwa, R. Grondin, PMU configuration for system dynamic performance measurement in large multiarea power systems, IEEE Trans. Power Syst. 17 (2002) 385–394.
[9] I. Kamwa, R. Grondin, Y. Hebert, Wide-area measurement based stabilizing control of large power systems—a decentralized/hierarchical approach, IEEE Trans. Power Syst. 16 (2001) 136–153.
[10] D. Karlsson, Convener, CIGRE Task Force 38.02.19, System protection schemes in power networks, CIGRE Technical Brochure, No. 187, 2001.
[11] D. Karlsson, M. Hemmingsson, S. Lindahl, Wide area system monitoring and control, IEEE Power Energy Mag. 2 (2004) 68–76.
[12] C.W. Liu, M.Ch. Su, S.-S. Tsay, Y.J. Wang, Application of a novel fuzzy neural network to real-time transient stability swings prediction based on synchronized phasor measurements, IEEE Trans. Power Syst. 14 (1999) 685–692.
[13] Manitoba HVDC Research Centre, PSCAD/EMTDC power system simulation software tutorial manual, 2003.
[14] A.R. Messina, J.M. Ramírez, J.M. Cañedo, An investigation on the use of power system stabilizer for damping inter-area oscillations in longitudinal power systems, IEEE/PES Winter Meeting, New York, NY, February 1997, Paper 94SM 532-2.
[15] M. Pavella, D. Ernst, D. Ruiz-Vega, Transient Stability of Power Systems: A Unified Approach to Assessment and Control, Kluwer Academic Publishers, Dordrecht, 2000.
[16] PEPITo user's manual, 2004, ⟨www.pepite.be⟩.
[17] A.G. Phadke, Synchronized phasor measurements in power systems, IEEE Comput. Appl. Power 6 (1993) 10–15.
[18] S. Rovnyak, C.-W. Liu, J. Lu, W. Ma, J. Thorp, Predicting future behavior of transient events rapidly enough to evaluate remedial control options in real time, IEEE Trans. Power Syst. 10 (1995) 1195–1203.
[19] C. Taylor, Convener, CIGRE Task Force 38.02.17, Advanced angle stability controls, CIGRE Technical Brochure, No. 155, 2000.
[20] Y.J. Wang, C.W. Liu, C.H. Liu, A PMU based special protection scheme: a case study of Taiwan power system, Electr. Power Syst. Res. 27 (2005) 215–223.
[21] L. Wehenkel, D. Ruiz-Vega, D. Ernst, M. Pavella, in: S. Savulescu (Ed.), Preventive and Emergency Control of Power Systems in Real Time Stability in Power Systems—Techniques for Early Detection of the Risk of Blackout, Springer, Berlin, 2005, pp. 199–232.

Alberto DEL ANGEL-HERNANDEZ was born in Mexico in 1972. He received the electrical engineering degree from the Veracruz Institute of Technology in 1994 and the M.S.E.E. degree from National Polytechnic Institute (Mexico) in 1999. From 1998 to 2001, he has been with the National Polytechnic Institute of Mexico, where he was a lecturer in the Department of Electrical Engineering. Presently, he is finishing PhD thesis at the Department of Electrical Engineering and Computer Science in the University of Liège, Belgium. His research interests include analysis of power system transient stability and automatic learning.

Pierre GEURTS graduated as an Electrical Engineer (in computer science) in 1998 and received the Ph.D. degree in applied sciences, in 2002, both from the University of Liège, Belgium. He is currently a research associate at the Belgian Fund for Scientific Research (F.N.R.S.). His research interests include machine learning and its applications in various fields, in particular bioinformatics.

Damien ERNST graduated as an Electrical Engineer in 1998 and received the Ph.D. degree in applied sciences, in 2003, both from the University of Liège, Liège, Belgium. He was a Research Fellow (1999-2003) and a Post-doctoral Research Fellow (2003-2006) of the FNRS at the University of Liège. He is currently an Assistant Professor at Supelec, Rennes, France. His research interests include optimal control, reinforcement learning, and power system control and optimization.

Mevludin GLAVIC received M.Sc. and Ph.D. degrees from the University of Belgrade, Serbia, and the University of Tuzla, Bosnia, in 1991 and 1997, respectively. As a postdoctoral researcher, within the Fulbright Program, he spent academic year 1999/2000 at the University of Wisconsin-Madison, USA. Since 2001, he is a Senior Research Fellow in the Department of Electrical Engineering and Computer Science at the University of Liége, Belgium (from December 2005 until September 2006 supported by Belgian National Fund for Scientific Research, FNRS). His research fields of interest include power system control and optimization.

Louis WEHENKEL graduated as an Electrical Engineer (in electronics) in 1986 and received the Ph.D. degree and the "Agrégation de l'Enseignement Supérieur" from the University of Liège, in 1990 and 1994, respectively. Currently, he is Professor in the Department of Electrical Engineering and Computer Science at the University of Liège. His research interests include stochastic methods, in particular optimization, automatic learning and data mining, and their application in power systems and in bioinformatics.